

## Numerical determination of 3D temperature fields in steel joints

Jean-Marc Franssen<sup>†</sup>

University of Liège, 1, Chemin des Chevreuils, 4000, Liege 1, Belgium

### Abstract

A numerical study was undertaken to investigate the temperature field in steel joints and to compare the temperatures in the joints with the temperatures of the adjacent steel members on the hypothesis that the thermal protection is the same on the joint and in the members.

Very brief information is given on the numerical model, supplemented with parametric studies made in order to determine the required level of discretization in the time and in the space domain. A simplified assumption for representing the thermal insulation is also discussed and validated.

Different numerical analyses are performed, with a variation of the following parameters: (i) type of joints, from very simple to more complex configurations, with welds and/or bolts, all of them representing joints between elements located in the same plane; (ii) unprotected joints or protected by one sprayed material; (iii) ISO, hydrocarbon or one natural fire scenario.

The fact that the thermal attack from the fire might be less severe because the joints are usually located in the corner of the compartment is not taken into account.

**Keywords** : temperature; steel; joints; numerical analysis; 3D

### 1. INTRODUCTION

It is usually assumed that the joints in steel construction do not require any special verification if their thermal insulation is at least equal to the insulation applied on the adjacent members. For example, a recent draft of Eurocode 3 [1] discusses connections:

The resistance of category A and B connections may be assumed to be sufficient provided that the two following conditions are met:

1. The thermal resistance  $(d_f/\lambda_f)_c$  of the fire protection of the connection is not less than the minimum value of the thermal resistance  $(d_f/\lambda_f)_m$  of the fire protection of any of the steel members joined by that connection, where:

$d_f$  is the thickness of the fire protection material—take  $d_f = 0$  for unprotected members;  $\lambda_f$  is the effective thermal conductivity of the fire protection material.

2. The utilization  $E_{d,ff}/R_d$  of the connection is not higher than the maximum value of the utilization of any of the steel members joined by that connection.

Also, concerning member verification, states [1]:

Net-section failure at fastener holes need not be considered, provided that there is a fastener in each hole, because the steel temperature is lower at connections due to the presence of additional material.

The assumption behind these rules is clearly that the temperature in the joint will be lower than the temperature in the members because there is a higher mass concentration in the joint. In fact, the local massivity, i.e. the ratio between the mass and the exposed surface, is the leading parameter rather than the mass. A numerical study was thus undertaken to see whether the assumption of a lower temperature in the joints is systematically valid.

## 2. SCOPE

Only steel connections are considered, i.e. no concrete slab is present. Three fire scenarios are considered, namely the ISO 834 fire curve, the hydrocarbon fire curve and one natural fire curve taken from Eurocode 1 [2] with a heating phase duration of 31 min and a maximum temperature of 773°C. Each joint is analyzed as unprotected, then as thermally protected.

## 3. HYPOTHESES

The thermal properties of steel are taken from Eurocode 3 [3]. The boundary conditions are taken from Eurocode 1 [2], i.e.  $h = 25$  W/mK for convection and  $\epsilon^* = 0.50$  for radiation.

Thermal contact is assumed to be perfect between any two adjacent objects; there is no thermal resistance produced by an eventual imperfect contact.

The temperature field is determined with the software SAFIR [4], using linear finite elements and an Euler-backward implicit time integration scheme ( $\theta = 0.90$ ).

## 4. PRELIMINARY STUDY ON THE DISCRETIZATION

It is important to know the required level of refinement in the discretization, both in time as well as in the space domain; the precision must not deteriorate excessively by too crude an approximation, but the calculation time has to be maintained within reasonable limits. Figure 1, for example, shows the isotherms after 30 min of ISO fire in a bolt passing through a 40 mm steel plate (the head and the screw are hexagonal, and the extremity of the cylindrical shank has also been approximated as hexagonal, which allows a 30° sector to be discretized). Figure 2 shows that a very similar temperature pattern can be obtained with a cruder discretization in which each extremity of the bolt is represented by a single finite element. On the other hand, if the bolt is not represented at all and only the steel plate is represented, the hot spot that appears near the bolt in Figures 1 and 2 will not appear and this cannot be accepted.

*Figure 1. Fine discretization for a bolt.*

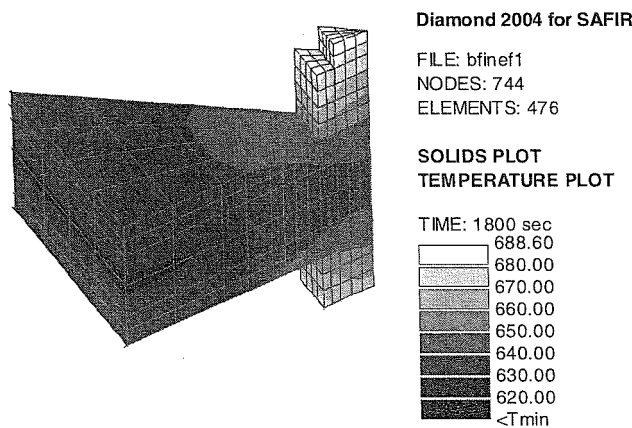
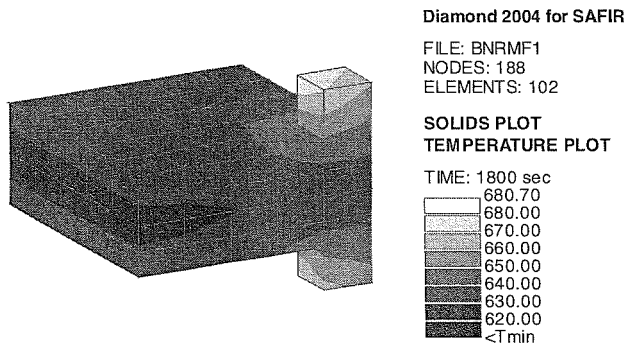


Figure 2. Discretization used for a bolt.



A simplified modelling is also proposed for the protection, that allows a significant reduction in the time for calculation, but above all in the time required for discretization. This simplification is explained here in a 2D situation for simplicity.

The most general way to take the thermal insulation into account is to represent it explicitly by some layers of finite elements (Figure 3). Of course, this requires a large number of additional finite elements and this has severe consequences on the time required for calculation but even more on the time required for building the model. In fact, if the thermal protection is provided by a lightweight material with a negligible specific heat, the thermal resistance  $R$  provided by the layer of insulating material can be evaluated, in the uniaxial situation that prevails for most parts of the steel sections, by the following equation:

$$R = \frac{1}{\alpha_p} + \frac{t_p}{\lambda_p} \quad (1)$$

where  $t_p$  is the thickness of the protection layer,  $\lambda_p$  is the thermal conductivity of the protection material and  $\alpha_p$  is the coefficient of heat exchange at the surface of the protection, see Equation (2).

$$\alpha_p = h_p + \varepsilon_p^* \sigma_0 (T_g^3 + T_g^2 T_p + T_g T_p^2 + T_p^3) \quad (2)$$

where  $h_p$  is the coefficient of convection,  $\varepsilon_p^*$  the relative emissivity,  $\sigma_0$  the Stefan-Boltzman constant,  $T_g$  the temperature of the gas and  $T_p$  the temperature at the surface of the protection. In fact, it can be shown that in most commonly used thermal protections, the surface resistance is negligible in Equation (1) when compared with the resistance to conduction provided by the thermal protection. Equation (3) is therefore a good approximation of Equation (1); replacing Equation (1) by Equation (3) amounts to assuming that the temperature at the surface of the insulation is equal to the temperature of the gas.

$$R = \frac{t_p}{\lambda_p} \quad (3)$$

In an unprotected section, the surface resistance on the steel plate  $1/\alpha_s$  is the only thermal resistance with  $\alpha_s$  given by Equation (4).

$$\alpha_s = h_s + \varepsilon_s^* \sigma_0 (T_g^3 + T_g^2 T_s + T_g T_s^2 + T_s^3) \quad (4)$$

It is therefore possible to consider the effect of the insulation and yet to represent only a non-insulated section (Figure 4), provided that the surface properties of steel are adapted accordingly. The simplest solution is given by Equations (5) and (6).

$$\varepsilon_s^* = 0 \quad (5)$$

$$\frac{1}{h_s} = \frac{t_p}{\lambda_p} \quad (6)$$

Figure 3. Protection represented.

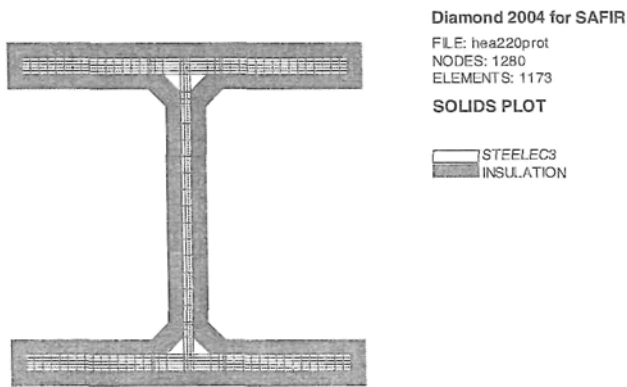


Figure 4. Equivalent protection.

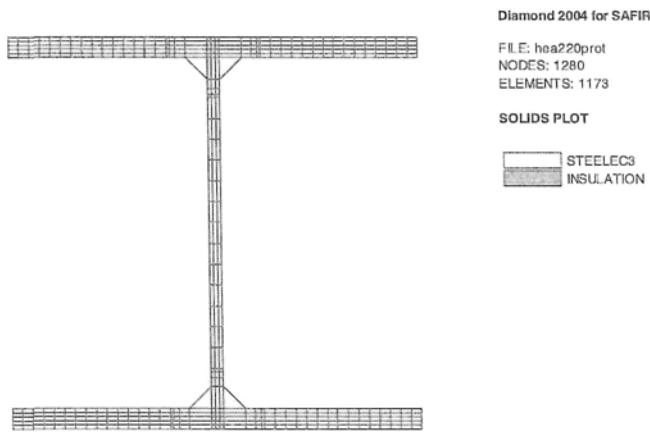
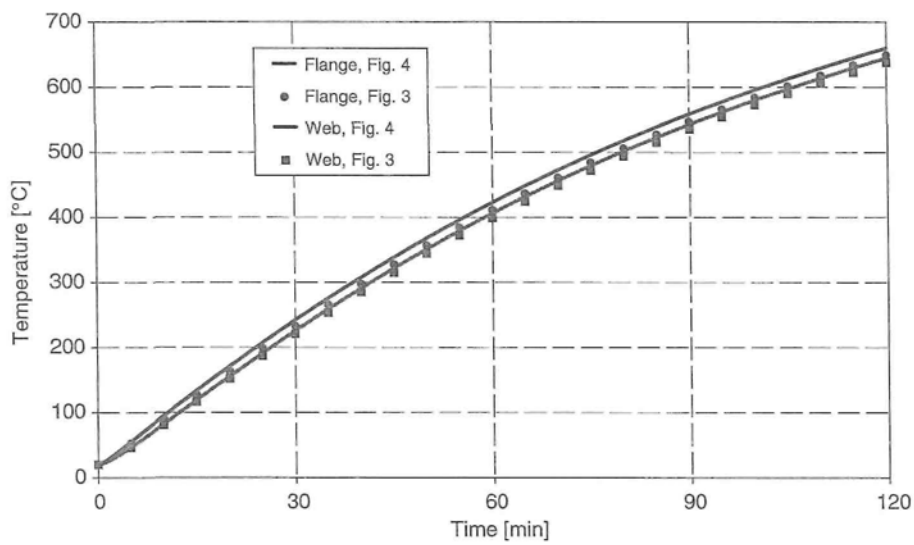


Figure 5. Comparison between represented protection and equivalent protection.



For example, in order to model a 10 mm layer of insulation with a thermal conductivity  $\lambda_p = 0.04$  W/mK, it is possible to use an unprotected section with an emissivity equal to 0 and a convection factor equal to  $4$  W/m<sup>2</sup>K. This has been done for the HEA220 represented in Figures 3 and 4 and the comparison in the temperatures obtained is given in Figure 5.

As far as the time step is concerned, it was shown by comparison with a very small time step that the relative error in the temperature does not exceed 0.5% with a rather large time step of 60s in a protected joint and 12s in an unprotected joint. The relative temperature difference between two different locations in a joint is not influenced by the time step.

## 5. FIN EFFECT FROM THE BOLT

A fin effect is produced when an object having a low mass but a high surface area is in contact with a massive object. It is sometimes referred to as the 'extended surface' effect. This effect is particularly used in the heat exchanger technology where a large number of thin plates are welded to the body that has to exchange heat as efficiently as possible with the environment; because of the high surface area of the plates and because of the low contact thermal resistance between the plates and the object, the heat exchange is increased by the plates.

In a joint submitted to the action of the fire, the bolts might play the role of fins for the plates that they are connecting. This effect is in fact visible in Figures 1 and 2. Under which conditions will this appear and how significant is this effect?

This effect has been analyzed in different geometrical configurations, different fire scenarios and different protection configurations. Figures 6 and 7, for example, refer to the situation after 20 min of ISO fire in an unprotected joint with an M27 bolt connecting two steel plates of 20 mm (Figure 6) and 8 mm (Figure 7). In each case, the length of the screw extending beyond the nut is 10 mm.

One temperature that is significant for the strength of the connection is the temperature in the shear plane in the bolt (node 168). This temperature of the bolt can be compared with the temperature in the plate as calculated away from the bolt, i.e. neglecting the influence of the bolt. It can be observed that the bolt on thick plates makes the temperature in the bolt higher than the temperature of the plate (Figure 6), whereas the same bolt on thin plates makes the temperature in the bolt lower than the temperature in the plate (Figure 7). What was a fin for a massive object becomes a protection for the thin object.

From all the analyses performed, it appears that the significant parameter is the ratio  $d/2t$  between the diameter of the screw and the total thickness of plates; for  $d/2t < 1$ , the bolt is a hot spot whereas, for  $d/2t > 1$ , the bolt is a cold spot.

Although the second situation might not be the most common one, it is acceptable in this case to neglect the effect of the bolt when evaluating the temperature, because this is on the safe side.

**Figure 6.** M27 bolt on  $2 \times 20$  mm plates.

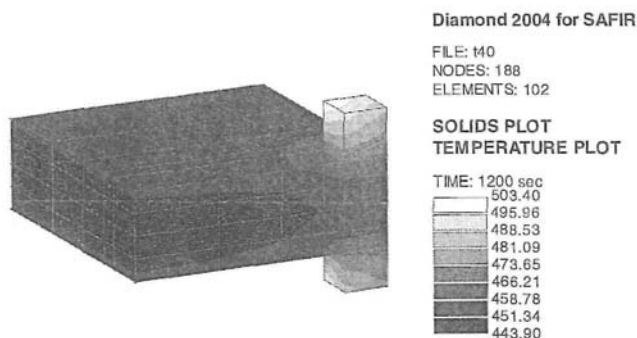


**Figure 7.** M27 bolt on  $2 \times 8$  mm plates.

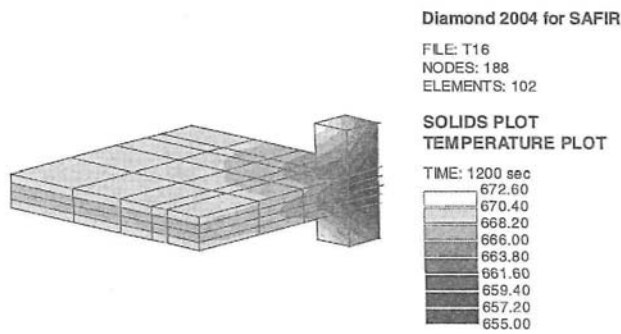
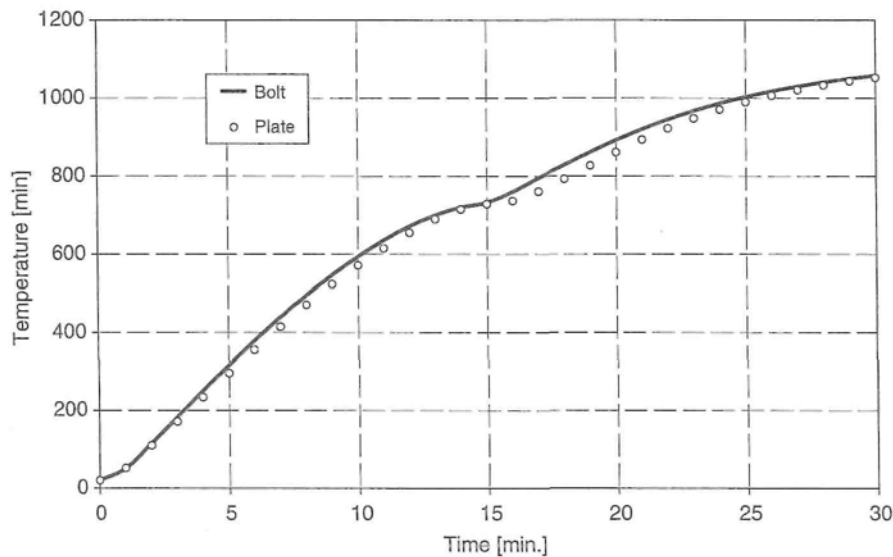


**Figure 8.** M27 on  $2 \times 20$  plates—hydrocarbon fire.



For the first situation, must the local effect of the bolt be taken into account? In fact, it appears that the local increase of temperature caused by the presence of the bolt is quantitatively very limited. This is shown in Figure 8 that represents the evolution of the temperature in the centre of the bolt (node 168, see Figure 6) and of the temperature in the centre of the plate far away from the bolt. This figure has been drawn for the case in which the highest differences can be observed, namely in an unprotected joint, with the very fast hydrocarbon fire curve and with an excessively long screw extending 40 mm beyond the nut. The amount by which the temperature is underestimated if calculated with the massivity of the two plates is very limited, with a peak value for  $\Delta T$  of 36°C after 18 min. For any other time within the fire or any other configuration, the difference would be less than 36°C. By configuration, we refer here to the combination fire-protection-geometry.

The effects of the configuration on the fire effects are:

- The faster the fire, the more pronounced the fin effect; with slower fires, time has a tendency to render the temperature field more homogeneous. This is why the effect is more pronounced with a hydrocarbon fire than with the ISO fire.
- The effect is reversed during the cooling down phase of a natural fire; if the fin effect is increasing the heat exchange with the environment, it will accelerate the heating as well as the cooling and, hence, a hot spot during heating will turn to a cold spot during the cooling.
- Thermal protection, because it slows down the temperature elevation, has also a tendency to render the situation more homogeneous.
- An excessively long screw will emphasize the fin effect on massive objects and the protection effect of thin objects.

According to the above considerations, it appears that the local effect of the bolts can really be neglected when evaluating the temperature distribution in a joint.

## 6. EFFECT OF THE WELDS

A geometry commonly encountered in joints is one in which a stiffener is made of a thin plate welded to a thicker plate. The weld in this case has several different effects: (a) it decreases locally the area of the surface that is exchanging heat with the environment, (b) it increases locally the mass of material to be heated, (c) it increases the surface available for the heat to pass by conduction from the thin plate to the thick plate.

The influence of the weld can also be analyzed in a 2D model (see Figures 9-11). They refer to a 20 mm thick plate (half thickness represented here for symmetry reasons) welded to a 40 mm plate with a 5 mm weld. The fire is the hydrocarbon fire and the section is not thermally protected. The figures seem to indicate that a very fine discretization is not really required, but that the weld absolutely has to be taken into account. In fact, the difference in temperatures between Figures 10 and 11 is not quantitatively so important and a discretization without the weld could represent an acceptable approximation.

## 7. TEMPERATURE OF THE WELD

Figure 12 refers to the same geometry as seen in Figure 9, but now for an ISO fire. The upper curve shows the temperature evolution as calculated by SAFIR in the thin plate far away from the connection. It can be observed that the curve corresponds exactly to the curve that is calculated with the simple equation of Eurocode 3 on the hypotheses of a uniform temperature in this plate. The same holds for the lower curve that depicts the evolution in the thick plate. The central curve corresponds to the temperature in the weld. It is closer to the temperature of the thick plate than to the temperature of the thin plate. It would be very uneconomical to design the weld based on the temperature of the thin plate, yet unsafe to design on the basis of the temperature in the thick plate.

A good and safe approximation is obtained if one considers the thermal massivity in this region as the one being calculated on the hypothesis of Figure 13A where a unit length is considered in each direction from the weld. The massivity is then calculated according to Equation (7).

$$\frac{A_m}{V} = \frac{6}{t_1 + 2t_2} \quad (7)$$

In this particular case, Equation (7) yields  $A_m/V = 6/(0.02 + 2 \times 0.04) = 60 \text{ m}^{-1}$  and it can be observed in Figure 12 that the temperature calculated on the basis of this thermal massivity is an acceptable approximation of the numerical solution.

Figure 9. Fine discretization.

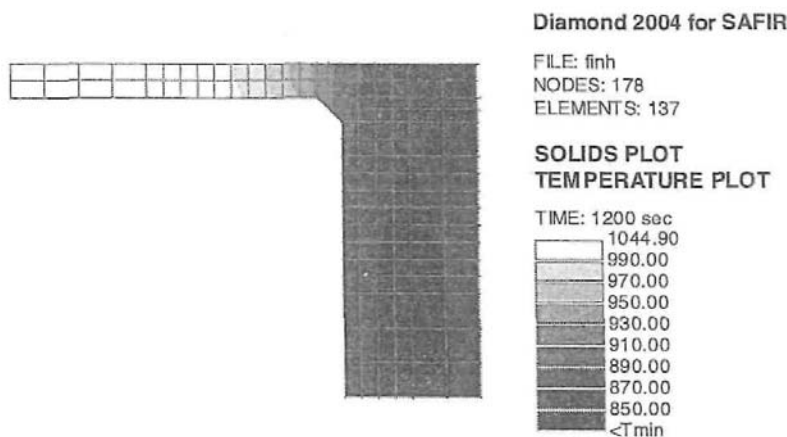


Figure 10. Normal discretization.

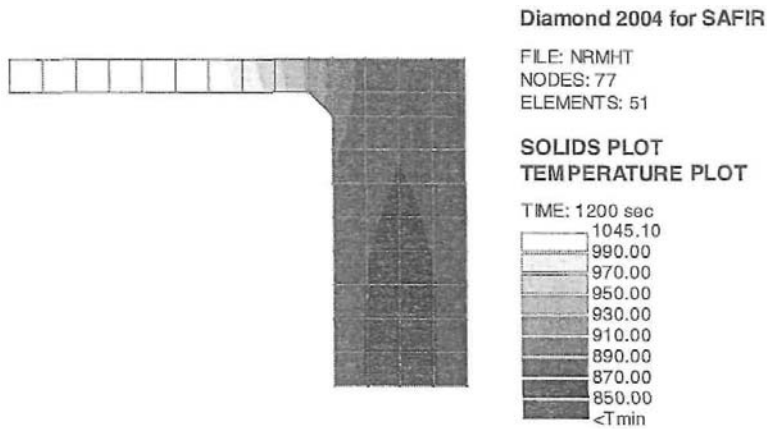


Figure 11. Weld not represented.

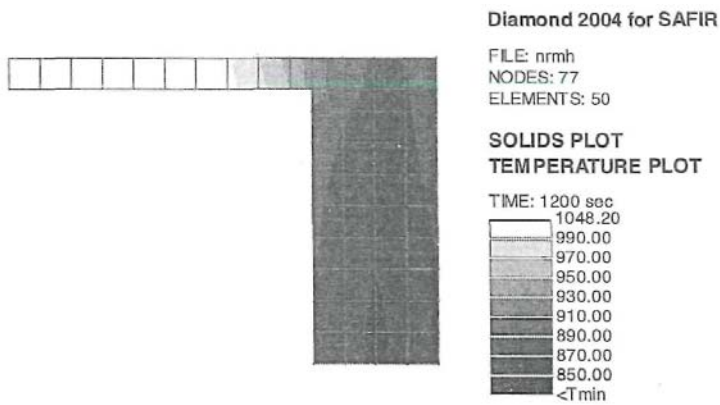
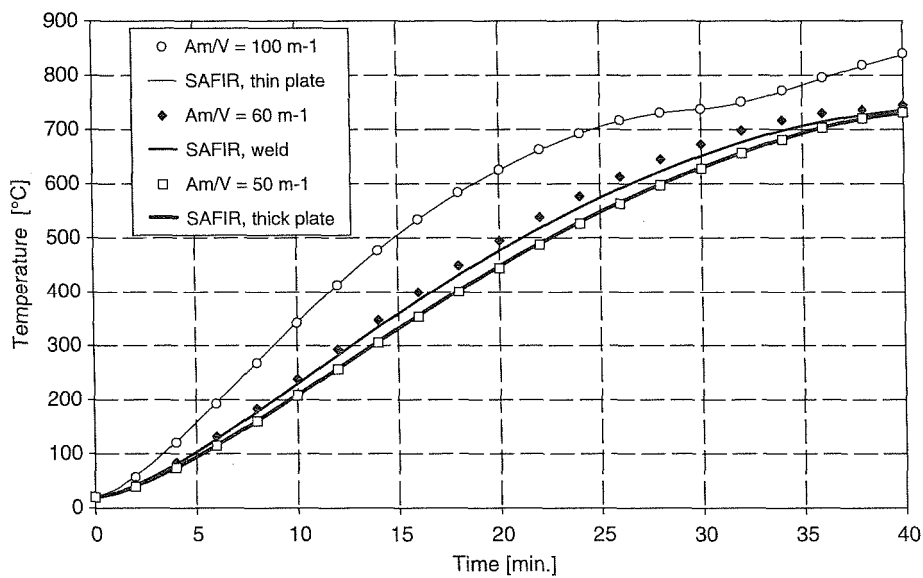
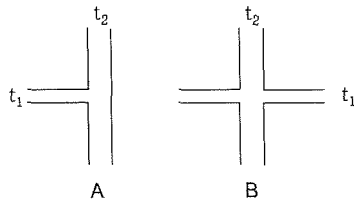


Figure 12. Evolution of the temperature under ISO fire.





**Figure 13.** Two different configurations.



In the geometrical configuration depicted by Figure 13B, the temperature in the weld is somewhat higher. It can be safely estimated on the basis of the thermal massivity evaluated by Equation (8).

$$\frac{A_m}{V} = \frac{8}{2t_1 + 2t_2} = \frac{4}{t_1 + t_2} \quad (8)$$

In this case, it yields  $A_m/V = 4/(0.02 + 0.04) = 67\text{m}^{-1}$ .

In fact, a more precise equation could be written instead of Equation (7). Changing the coefficient applied to  $t_2$  in this equation from 2 to 9/4 yields as a consequence that the temperature of the weld is the same as the temperature of the thick plate if  $t_1 = 0.75 t_2$  as observed in the numerical calculations. In this case, this would lead to  $A_m/V = 55 \text{ m}^{-1}$  for the weld and the temperature calculated by the simple method would be somewhat colder, in fact nearly exactly the same as the temperature calculated by SAFIR. The expression of Equation (7) has been kept for simplicity.

## 8. 3D ANALYSES

### 8.1. Bar in tension—one cover plate

Figure 14 shows the isotherms in an unprotected tension joint with one single cover plate after 30min of ISO fire. The bars to be joined have a  $12 \times 150 \text{ mm}^2$  section and the 12mm thick cover sheet is 352 mm long. One quarter of the joint only has been analyzed for symmetry reasons; in fact, a total of eight bolts is used in the joint.

In this case, the ratio between the diameter of the bolt and the thickness of the plate is equal to 20/24 and, as it is smaller than 1, the bolts create a hot spot in the joint.

The temperature after 30 min calculated by the simple method using the thermal massivity of the tension plates  $A_m/V = 2(0.012 + 0.150)/(0.012 \times 0.150) = 180\text{m}^{-1}$  is equal to  $806^\circ\text{C}$ , whereas the temperature calculated with the thermal massivity of the joint (neglecting the effect of the bolts)  $A_m/V = 2(0.150 \times 0.352 + 0.024 \times 0.352 + 0.150 \times 0.012)/(0.024 \times 0.150 \times 0.352) = 100 \text{ m}^{-1}$  is  $738^\circ\text{C}$ . These two significant temperatures are represented on the temperature scale on the right in Figure 14. It can be observed in this unprotected connection that:

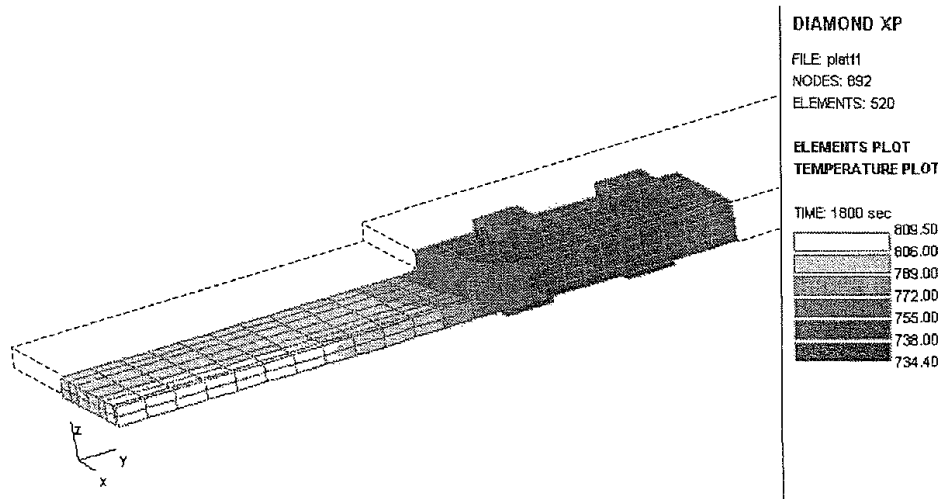
1. The joint is definitively colder than the tension plates.
2. The colder zone in the tension plates near the joint has a limited extent.
3. Nearly the whole joint has a temperature that is by  $20^\circ\text{C}$  in excess of the temperature that is calculated by the simple method using the massivity of the joint.

Figure 15 refers to the same joint, now thermally protected. The temperatures calculated by the simple method after 90 min of exposure are  $523^\circ\text{C}$  in the tension bars away from the joint and  $367^\circ\text{C}$  in the joint. From the isotherms on the figure, it can be observed that:

1. The joint is still colder than the tension plates.
2. The colder zone in the tension plates near the joint extends a longer distance.
3. The temperature at any point in the joint is at least  $410^\circ\text{C}$ . The temperature in the bolt that is closest to the bars is  $425^\circ\text{C}$ . This means that the temperature in the joint is  $40^\circ$  to  $60^\circ\text{C}$  higher than temperature that is calculated by the simple method using the massivity of the joint.

The observations that have been made here in the simplest case of a joint with two different thicknesses, and the difference between the insulated or non-insulated joint, will in fact generally be observed in all the more complex geometries that can be analyzed. This is illustrated in the next sections.

**Figure 14.** Bars in tension—one cover plate—unprotected.



### 8.2. Bars in tension—two cover plates

Figure 16 is a joint for the same bars as presented in Figure 14, i.e. non protected, but now with two symmetrically located cover plates with a thickness of 6 mm each. The same observations can be made here, namely; a cold zone of limited extent in the bar close to the joint; a joint that is significantly colder than the bar; the temperature in the joint somewhat higher than the temperature of 738°C that can be calculated by the simple method on the basis of the massivity of the joint.

### 8.3. Bars in tension—net or whole section

It is written in Eurocode 3 [1] that net-section failure at fastener holes need not be considered because of the presence of additional material.

Figure 17 shows the evolution of the temperature in the thermally protected joint depicted in Figure 16 at the level of the bolt, first as calculated by SAFIR, then as calculated on the basis of the local massivity in the joint,  $97 \text{ m}^{-1}$ , and it is seen that this is unsafe, and finally on the basis of the massivity of the connected bars,  $180 \text{ m}^{-1}$ , and it is seen that this is safe.

Figure 18 shows the evolution of the tension strength in the bar, first according to the temperature computed by SAFIR and considering the net section of  $12 \times 110 = 1320 \text{ mm}^2$ , then calculated on the basis of the simple temperature in the bar and on the gross section of  $12 \times 150 = 1800 \text{ mm}^2$ .

It can be observed that the procedure recommended by Eurocode to neglect the reduction in section of the bars at the locations of the fasteners is not safe when the simply calculated temperature is not sufficiently higher than the 'true' temperature, namely during the first moments of the fire (90min for the case of Figure 18) and also for longer durations when the temperatures in the whole structure tend to level off to a uniform level because of the tendency of nominal fire curves to end up in a quasi steady state constant temperature (not seen in Figure 18).

Figure 15. Bar in tension—one cover plate—thermally protected.

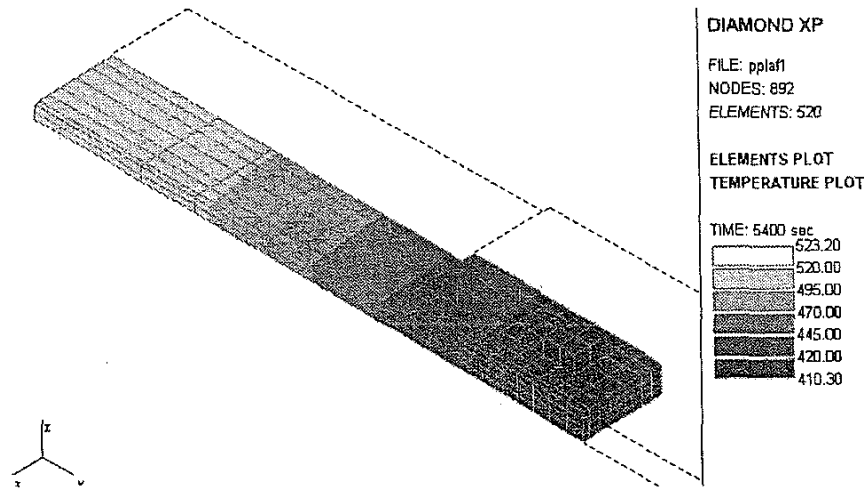


Figure 16. Bars in tension—two cover plates—unprotected.

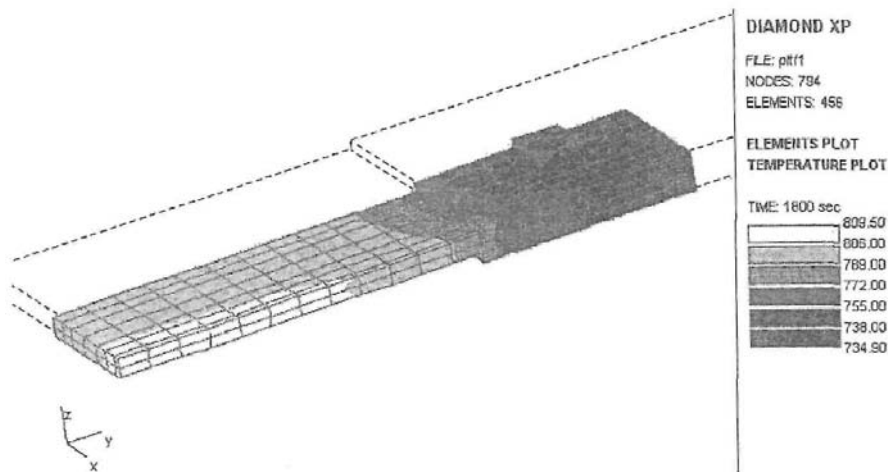
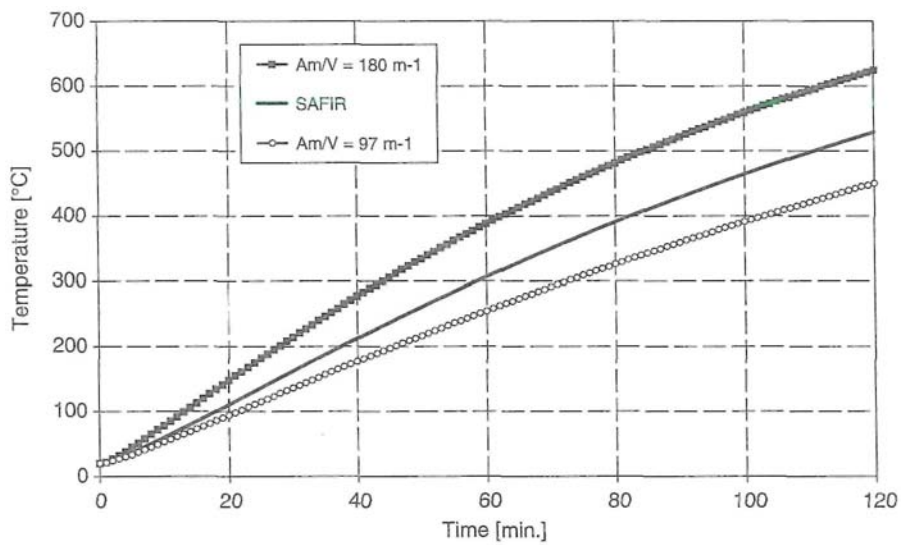
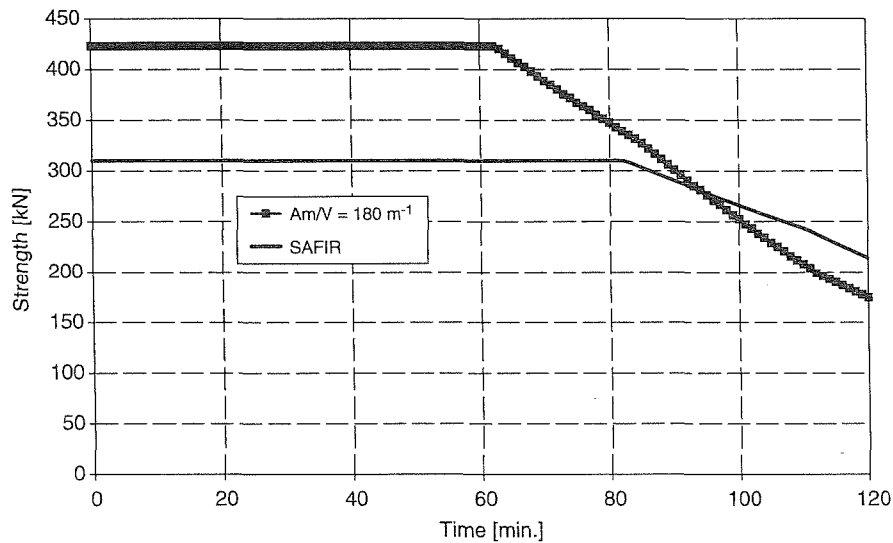


Figure 17. Evolution of the temperature in the protected joint.



**Figure 18.** Evolution of the strength in the protected joint.



#### 8.4. Beam in bending—cover plates

Figure 19 shows 1/8 of a thermally protected joint in an IPE 330 steel beam submitted to bending and to shear. The joint is made of 20 mm bolts and 6 mm thick steel plates.

If calculated by the simple method based on the local massivity, the temperatures after 90 min of ISO fire are:

- 552°C in the steel beam ( $A_m/V = 200 \text{ m}^{-1}$ )
- 400°C in the cover plates on the flanges ( $A_m/V = 114 \text{ m}^{-1}$ )
- 373°C in the cover plates on the web ( $A_m/V = 103 \text{ m}^{-1}$ )

As in the geometrical simpler joint of Figure 15, the temperature in this joint is in fact colder than the temperature calculated in the element by the simple method, but the temperature in the different parts of the joint is significantly higher than the temperature calculated on the basis of the local massivity. It can even be observed that the temperature in the plates covering the web is higher than the temperature in the plates covering the flange, whereas the local massivity should indicate the contrary; this is of course because of the influence of the thin web that is surrounding this part of the joint.

The same holds for the unprotected beam (Figure 20); the temperatures in the joint are higher than the temperature calculated on the basis of the local massivity, namely 633°C in the plates on the web and 654°C in the plates on the flange.

#### 8.5. Beam in bending—flush end plates

Figure 21 shows two IPE360 beams with welded flush end plates connected by 24 mm bolts. The steel plates are 20 mm thick and 20 mm wider in each transverse dimension than the beam section.

Calculated according to the simple method based on the local massivity, the temperatures after 20 min of ISO fire are:

719°C in the beam ( $A_m/V = 186 \text{ m}^{-1}$ ) 445°C in the plates ( $A_m/V = 50 \text{ m}^{-1}$ )

Here also, the temperature in the connection is lower than the simple temperature in the elements, but significantly higher than the temperature calculated by the simple method based on the local massivity.

**Figure 19.** Beam with cover plates—protected.

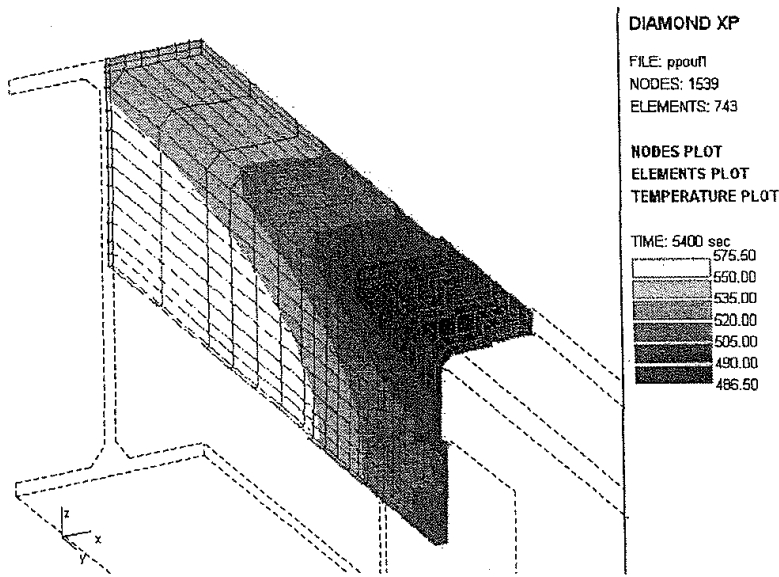
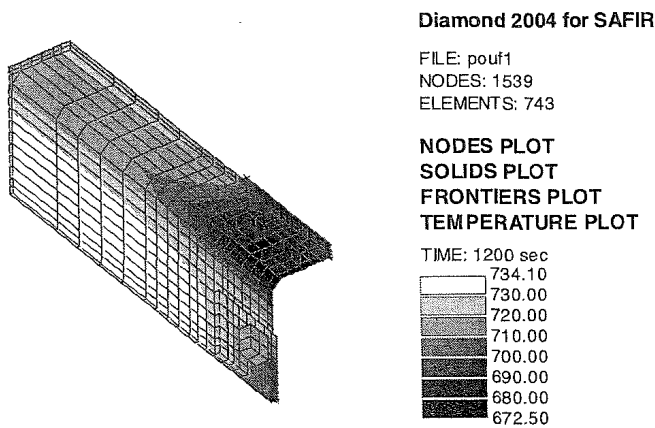


**Figure 20.** Beam with cover plates—unprotected.



### 8.6. Beam to column joint—flush end plates

Two IPE360 beams are connected by flush end plates to a HEA240 column. The joint is a moment resisting joint but no stiffener is provided. The end plates are 20 mm thick and 20 mm wider in each transverse dimension than the beam. 20 mm bolts are used to connect the end plates to the flanges of the column.

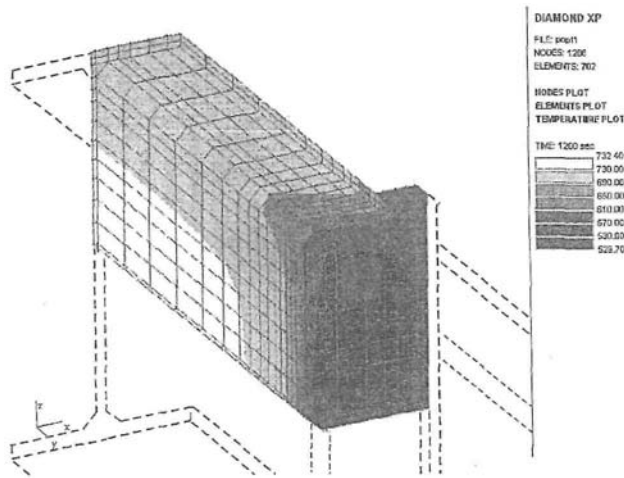
Figure 22 shows the isotherms after 120 min of ISO fire in 1/8 of the protected joint. Simply calculated temperatures are:

634°C in the beam ( $A_m/V = 186 \text{ m}^{-1}$ ) 621°C in the column ( $A_m/V = 178 \text{ m}^{-1}$ ) 389°C in the plates ( $A_m/V = 77 \text{ m}^{-1}$ )

It has to be noted that the local massivity calculated simply on the basis of the cumulative thickness of the plate and of the flange of the column would yield  $A_m/V = 2/0.032 = 63 \text{ m}^{-1}$  and a temperature of 340°C. Here, the local massivity has been evaluated on the basis of a horizontal section through these two plates, taking into account the additional lateral surfaces.

Here again, the temperature in the joint is lower than the temperature simply calculated in both connected members, but the temperature is higher than the temperature calculated on the basis of the local massivity.

**Figure 21.** Unprotected flush, end plate.



### 8.7. Beam to column joint—angles

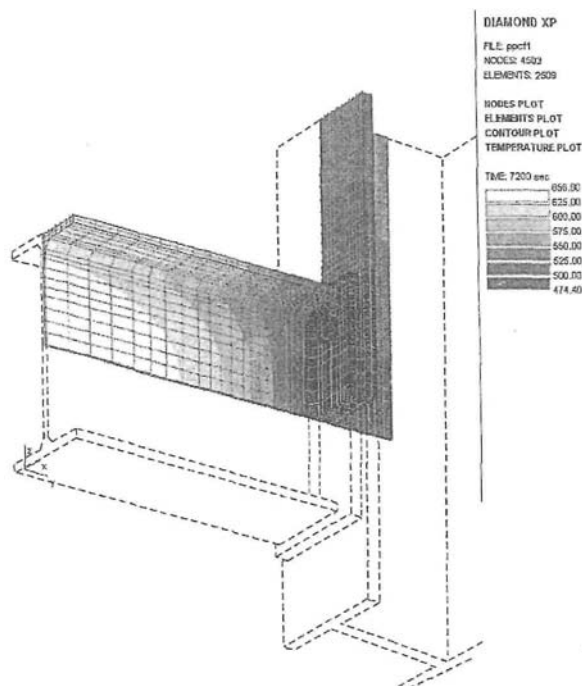
Figure 23 represents the isotherms after 20 min of ISO fire in an unprotected joint connecting the IPE360 beams to the HEA240 column. The bolts are M20. The angles or cleats are 14mm thick, 240 mm wide and 140/65 mm long.

Simply calculated temperatures are:

719°C in the beam ( $A_m/V = 186 \text{ m}^{-1}$ )

716°C in the column ( $A_m/V = 178 \text{ m}^{-1}$ )

**Figure 22.** Protected flush end plate.



### 8.8. Beam to column joint—flush end plate and stiffener

Figure 24 refers to a protected joint connecting the IPE360 beam with the HEA240 column with 24 mm thick flush end plates and 12.7 mm thick stiffeners between the flanges of the column.

Temperatures calculated by the simple method after 90 min of ISO fire in 1/8 of the protected joint are:

532°C in the beam ( $A_m/V = 186 \text{ m}^{-1}$ ) 520°C in the column ( $A_m/V = 178 \text{ m}^{-1}$ ) 269°C in the end plates ( $A_m/V = 64 \text{ m}^{-1}$ ) 485°C in the stiffeners ( $A_m/V = 157 \text{ m}^{-1}$ )

In this case, it is found that the temperature in the end plates is higher than the simply calculated temperature, but the temperature in the stiffener is lower than the simply calculated temperature.

### 8.9. Beam to column joint—angles and stiffener

Figure 25 is a joint between the IPE360 beams and HEA240 column made of bolted cleats and involving stiffeners between the flanges of the column. The thickness of the stiffener is 12.7 mm. The thickness of the cleats is 14 mm for the connection to the flanges of the beams and 10 mm for the connection to the web of the beams.

The figure shows the isotherms after 30min of ISO fire in this joint without thermal protection. They have to be compared with:

809°C in the beam ( $A_m/V = 186 \text{ m}^{-1}$ )

805°C in the column ( $A_m/V = 178 \text{ m}^{-1}$ )

732°C in the cleats on the flanges of the beam ( $A_m/V = 87 \text{ m}^{-1}$ )

792°C in the stiffeners ( $A_m/V = 157 \text{ m}^{-1}$ )

It has to be noted that the results of the simulation made on the two joints of Figures 24 and 25 have been compared with experimental results obtained by Kruppa [5]. The agreement was generally quite good, with a tendency for the experimental temperatures to be somewhat lower than the numerically calculated values in the joints, owing to a corner effect in the testing compartment. These comparisons cannot be shown here because of the limited amount of allocated space for each paper.

Figure 23. Unprotected joint with angles.

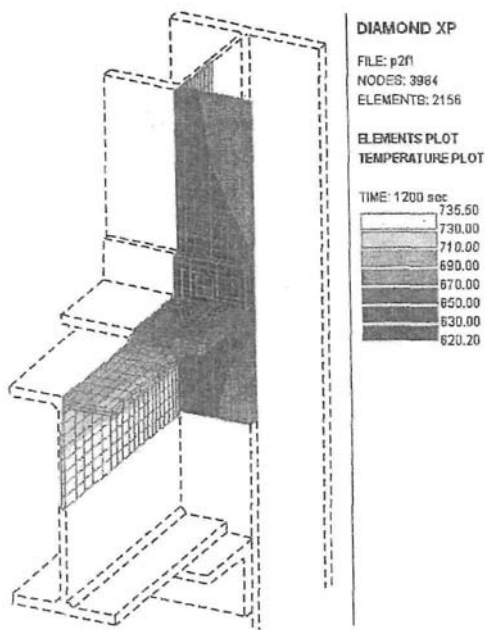


**Figure 24.** Protected joint with flush end plate and stiffeners.

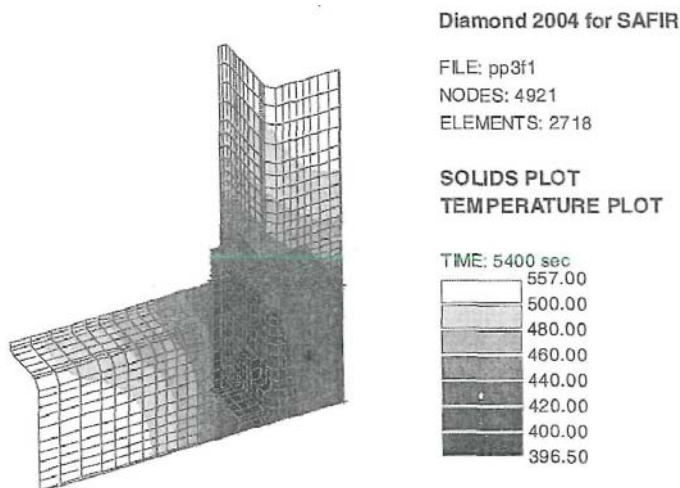
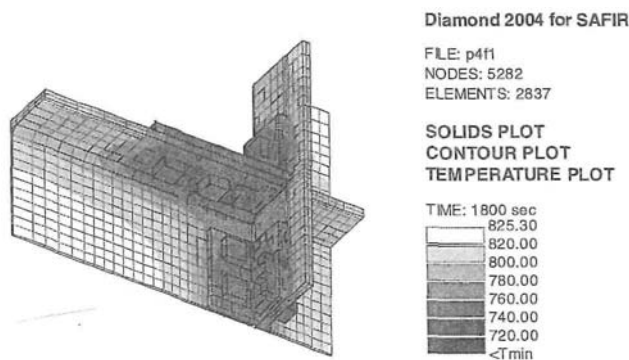


**Figure 25.** Unprotected joint with cleats and stiffener.



## 9. CONCLUSIONS

From all the examples that have been calculated, there has been no single occurrence where the temperature in the joint would have been higher than the temperature of the connected elements. This result was obtained although the favourable effect of colder temperatures in the corners of the compartment which can play a role in most of the cases has not been taken into account. It is therefore indeed safe to design the connection on the basis of the temperature calculated in the connected elements.

The recommendation of Eurocode 3 [1] that net-section failure at fastener holes need not be considered cannot be supported because, after an important duration of exposure to a fire curve that has a tendency to reach a nearly steady state condition—such as the nominal fire curves—there is a tendency for the temperature to become more and more uniform and, hence, the effect of additional material near the hole is very much diluted. Furthermore, this local effect of the fastener can be negative in some cases, namely when the diameter of the bolt is smaller than the total thickness of the plates that the bolt connects.

The recommendation that the temperature of a connection may be assessed using the local massivity values of the components comprising the connection can also not be supported. In nearly all calculated examples, the temperature in the components was higher than what the local massivity would have indicated. This is probably because the dimensions of the components are of an order of magnitude smaller than the dimensions of the connected members and the influence of these members is felt in the components.



## **REFERENCES**

1. Draft prEN 1993-1-2. *Eurocode 3: Design of Steel Structures—Part 1-2: General Rules—Structural Fire Design*. Third preliminary draft, May 2001.
2. ENV 1991-1-2. *Eurocode 1—Basis of Design and Actions on Structures—Part 2-2: Actions on Structures—Actions on Structures Exposed to Fire*.
3. ENV 1993-1-2. *Eurocode 3: Design of Steel Structures—Part 1-2: General Rules—Structural Fire Design*. CEN: Brussels, May 1995.
4. Franssen JM. *SAFIR. A Thermal/Structural Program Modelling Structures under Fire*. Proc. NASCC 2003, A.I.S.C. Inc., Baltimore, April 2-A (2003).
5. Kruppa J. *Résistance au Feu des Assemblages par Boulons Haute Résistance*. C.T.I.C.M.: Puteaux, France, June 1976.